LHCb 2003-115
15 September, 2003

LHCb Flavour Tagging Performance

Marta Calvi [1], Olivier Dormond [2] and Marco Musy [1]

([1]) *University of Milano-Bicocca and INFN, Milano, Italy*
([2]) *University of Lausanne, Lausanne, Switzerland*

Abstract

In CP violation measurements, the most accurate determination of the B flavour of neutral and charged B-mesons is necessary. In this note we summarize the tagging performances for the LHCb experiment, using different approaches and studying different decay channels.

1 Introduction

The identification of the initial flavour of reconstructed B^0 and B_s^0 mesons (flavour tagging) is necessary in order to study decays involving CP asymmetries and flavour oscillations.

The statistical uncertainty on the measured CP asymmetries is directly related to the effective tagging efficiency ε_{eff}, which is defined as

$$\varepsilon_{\text{eff}} = \varepsilon_{\text{tag}} D^2 = \varepsilon_{\text{tag}} (1 - 2w)^2 \,, \tag{1}$$

where ε_{tag} is the tagging efficiency (probability that the tagging procedure gives an answer), D is the dilution term, and w is the wrong tag fraction (probability for the answer to be incorrect when a tag is present). The probabilities ε_{tag} and w are calculated as

$$\varepsilon_{\text{tag}} = \frac{R + W}{R + W + U} \qquad w = \frac{W}{R + W} \,, \tag{2}$$

where R, W, U are the number of correctly tagged, incorrectly tagged, and untagged events, respectively.

In figure 1 the effective efficiency ε_{eff} is given as a function of the wrong tag fraction for different values of the tagging efficiency ε_{tag}. The goal of this study is to find the conditions to maximize the effective tagging efficiency and minimize in this way the statistical error on the measured asymmetries.

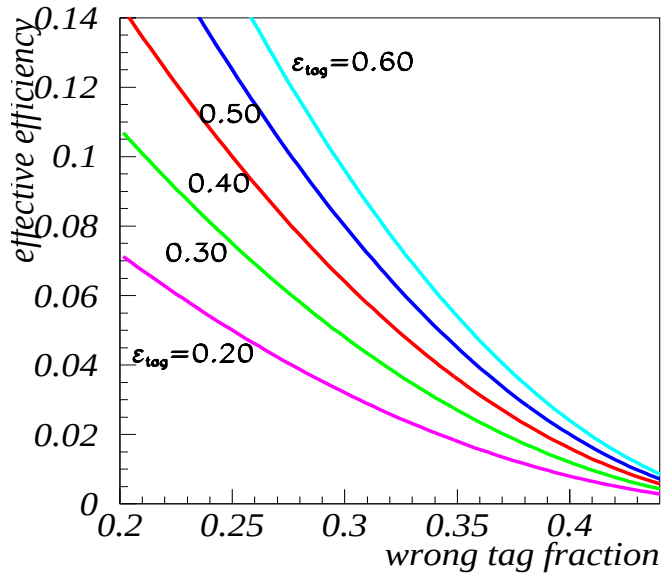

Figure 1: The effective efficiency ε_{eff} as a function of the wrong tag fraction w for different values of the tagging efficiency ε_{tag}.

2 Analysis framework

This study has been carried out in the analysis framework of the LHCb C++ object oriented software, using the programs Brunel v17r4 for the global event reconstruction and DaVinci v8r2 as the standard tool for the physics analysis. In particular, for the flavour tagging of the B hadron, a dedicated algorithm has been written.

Many exclusive decay channels of the B-hadron have been analysed in a realistic way, i.e. without looking at the Monte Carlo true information. Only the reconstructed information in the event is used at all steps of the analysis. The truth information has been used only to determine whether a tag is correct or not.

3 Particle identification and Event selection

For both event selection and flavour tagging, a positive particle identification is of paramount importance. This is provided by the two RICH devices of the LHCb detector, by the muon chambers and by the calorimetry system. The RICH systems give

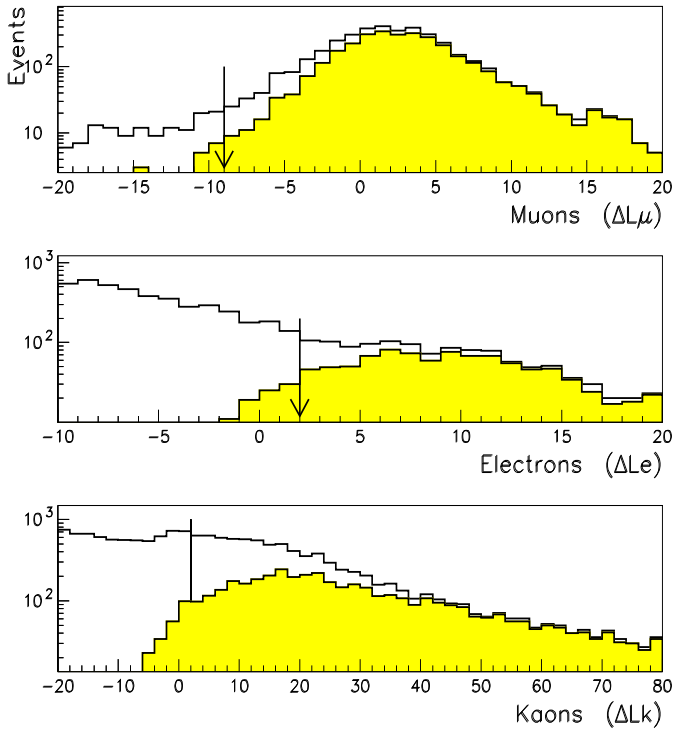

Figure 2: Log-likelihood distributions for tagging candidates (muons, electron and kaons, from top to bottom) in *selectable* $B_s^0 \to D_s^{\mp} K^{\pm}$ events. Shaded histograms are for true muons, electrons or kaons.

as output a set of probabilities for each single particle type hypothesis, which are then combined to give a "best" identification of a charged track. Examples of such likelihood

distributions are shown in Figure 2, where the shaded histogram is the likelihood for true muons, electrons or kaons, and the open histogram corresponds to the likelihood distributions for tracks which are not of that given type. The information of the RICH particle ID probability has been used to tune the particle ID cuts to have the best performance in the flavour tagging. The arrows indicate the cuts applied to maximize the final tagging efficiencies.

With these requirements, the ghost rate is only 2%, while purities for muons electrons and kaon are 83%, 80% and 89% respectively. Cut efficiencies are 89%, 85% and 61% respectively when considering, as a starting sample, *long* tracks of momentum $p > 5$ GeV.

Event selection in the various decay channels is provided by individual off-line selection algorithms. These selection algorithms have been used to derive final results on tagging performances. Nonetheless, in order to increase the selection efficiency, and reduce the statistical uncertainty, an alternative method has been considered which allows to select artificially the B-decay signal. It consists in taking the Monte Carlo tree of the signal B decay, and require that the counterpart of all tracks defining the decay channel have been reconstructed in the detector. In this case the event is *selectable*, although it is not necessarily selected as it may fail one or more of the off-line selection cuts. Results obtained on *selectable* events have been checked for consistency against the tagging outcome on the off-line selections. All figures shown in this note have been produced with *selectable* events.

4 Single particle tag

In the following sections two types of single particle tag algorithms will be described: opposite-side tag, based on muons, electrons and kaons, which are used to tag B^0 and B_s^0 mesons and same-side tag based on kaons which are used to tag B_s^0 mesons only.

Only *long* track particles have been considered as tag candidates. When more than one primary vertex is reconstructed in the event, all single particle tags are required to have an impact parameter significance in excess of 3.7 with respect to any primary vertex which was not chosen as the $b\bar{b}$ production vertex.

4.1 Opposite side tag

Opposite-side tag algorithms determine the flavour of the b-hadron accompanying the reconstructed B meson under study. They use the charge of the lepton from semileptonic b decay and of the kaon from the $b \to c \to s$ decay chain. They also use the charge of the inclusive secondary vertex reconstructed from b-decay products (see section 5). When the accompanying b hadron is a neutral B meson, due to the possibility of flavour oscillations all these methods have an intrinsic dilution.

To select opposite-side tag lepton candidates, a momentum $p > 5\,\mathrm{GeV}/c$ and $p_\mathrm{T} > 1.2\,\mathrm{GeV}/c$ are required, reducing the contribution from $b \to c \to \ell$ decays which tag the wrong charge. In case of multiple candidates, the one with highest p_T is chosen. Figure 3 shows the p_T distribution of the chosen candidate and the effective efficiency as a function of the p_T cut for opposite-side muon and electron tag candidates, respectively.

Considering a sample of $B^0_{(s)} \to h^+h^-$ events, once the B meson has been reconstructed in the event, which passed Level-0 and Level-1 trigger, the probability that a right tag

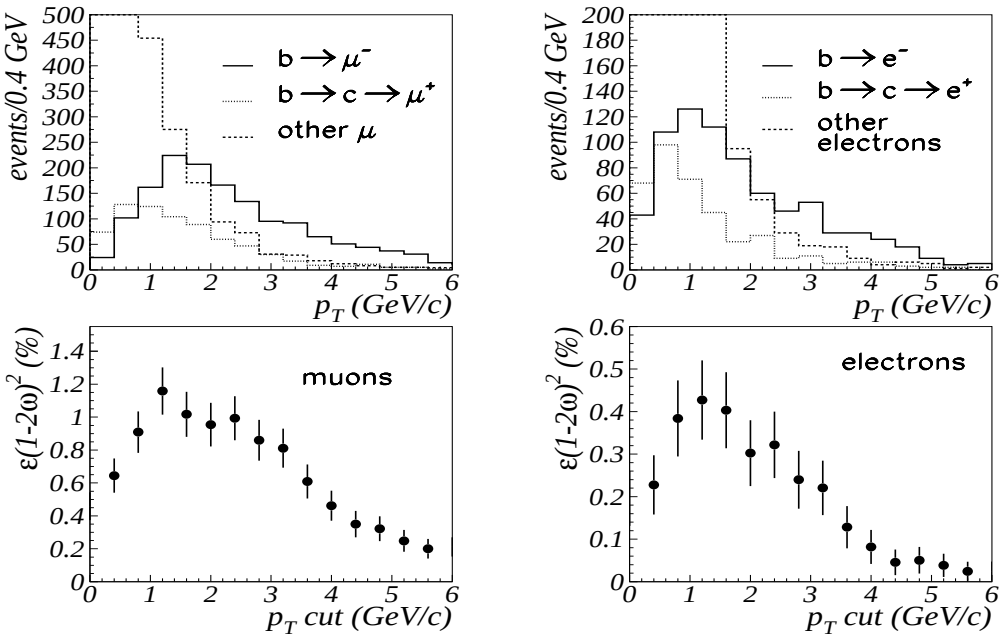

Figure 3: Upper plot: $p_{\rm T}$ distribution for opposite-side muon (left) and electron (right) tag candidates, having $p > 5\,{\rm GeV}/c$, after Level-0 and Level-1 trigger. In the "other muon (electron)" category also misidentified hadrons are included. Lower plots: effective efficiency as a function of the minimum $p_{\rm T}$ required. Events used are $\rm B_s^0 \to K^+K^-$.

lepton from a semileptonic decay of the opposite b-hadron is found in the detector acceptance ($15 < \theta < 250\,{\rm mrad}$) is 8.7% and 6.3% for muons and electrons, respectively. These numbers include the reduction due to the flavour oscillation of the opposite B-meson. The difference between muons and electron probabilities is induced by the trigger requirements. Table 1 shows the efficiencies for these particles to be reconstructed as a *long* track and correctly identified. The final probability for finding a right tag lepton from the semileptonic decay of the opposite b-hadron results 5.7% and 2.2% for muons and electrons, respectively.

Particle track	μ	e	K
has Velo hits	99%	99 %	91%
has T Station hits	96%	88 %	70%
is *long* track	93%	82 %	64%
has correct PID	86%	64 %	45%
pass tag cuts	66%	35 %	32%

Table 1: Efficiencies for selecting a tagging particle, when it exist in the detector acceptance, at different steps of the selection. The Velo hits and T Station hits requirements are independent, while the *long* track requirement implies the existence of both Velo and T Station hits.

To select opposite-side tag kaon candidates, a momentum $p > 3\,{\rm GeV}/c$, $p_{\rm T} >$

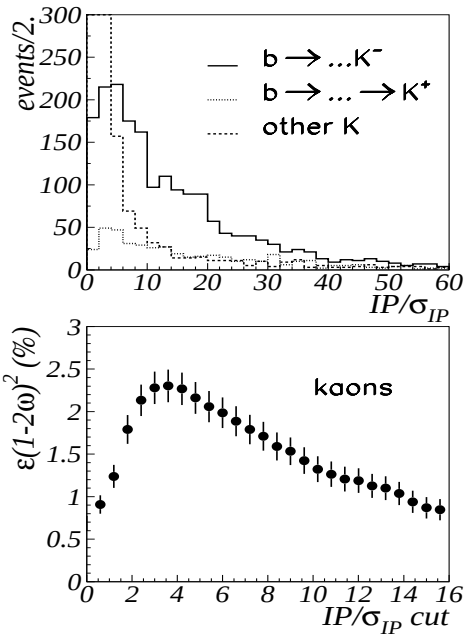

Figure 4: Upper plot: Distribution of the significance $\mathrm{IP}/\sigma_{\mathrm{IP}}$ for opposite-side kaon tag candidates, after p and p_{T} cuts have been applied and after Level-0 and Level-1 trigger. In the "other K" category also misidentified hadrons are included. Lower plot: effective efficiency as a function of the minimum $\mathrm{IP}/\sigma_{\mathrm{IP}}$ required. Events used are $\mathrm{B_s^0} \to \mathrm{K^+K^-}$.

$0.4\,\mathrm{GeV}/c$ and an impact parameter with respect to the primary vertex with significance $\mathrm{IP}/\sigma_{\mathrm{IP}} > 3.7$ are required. These cuts enhance the contribution of kaons from b decays with respect to kaons produced in the fragmentation. Fig. 4 shows the distribution of the significance $\mathrm{IP}/\sigma_{\mathrm{IP}}$ for opposite-side kaon tag candidates, after p and p_{T} cuts have been applied, and the effective efficiency as a function of the $\mathrm{IP}/\sigma_{\mathrm{IP}}$ cut.

About 33% of the triggered events have, in the detector acceptance, a kaon produced in the decay of the accompanying b hadron carrying the right tag charge. This number includes the reduction due to the flavour oscillation of the opposite B-meson. The momentum spectrum of these kaons is quite soft and about 16% of them decay before reaching the tracking chambers. The efficiencies for defining a tagging kaon, at various steps of the selection, are also shown in Table 1. The final probability for finding a right tag kaon from the decay of the opposite b-hadron is 11%.

μ origin	Fraction in sample	Wrong tag
$b \to \mu$	51%	7%
$b \to c(\bar{c}) \to \mu$	17%	12%
other μ	14%	7%
misidentified hadrons	18%	9%
total	100%	35%

Table 2: Composition of the selected muon sample and sources of wrong tag.

Electron origin	Fraction in sample	Wrong tag
$b \to$ e	46%	6%
$b \to c(\bar{c}) \to$ e	13%	11%
other electrons	19%	9%
misidentified hadrons	22%	10%
total	100%	36%

Table 3: Composition of the selected electron sample and sources of wrong tag.

K origin	Fraction in sample	wrong tag
$b \to ...K$	69%	16%
other K	21%	11%
misidentified hadrons	10%	5%
total	100%	32%

Table 4: Composition of the selected Kaon sample and sources of wrong tag.

Table 2, 3 and 4 indicate the composition of the selected samples of opposite-side muon, electron and kaon, respectively and the corresponding fractions of wrong tags.

For muons, the main part of wrong tags stems from cascade decays of the b-hadron, while for kaons, the larger sources are wrong sign kaons in the opposite b-hadron decay chain and kaons from other sources, in particular kaons from fragmentation. An intrinsic component of the mistag corresponds to events where the opposite b-meson oscillated.

4.2 Same side tag

Same side tags determine directly the flavour of the signal B meson exploiting the correlation in the fragmentation decay chain. It is used to tag B_s^0 mesons. If a B_s^0 ($\bar{b}s$) is produced in the fragmentation of a $\bar{b}$ quark, an extra $\bar{s}$ is available to form a K meson, which is a charged K in about 50% of the time and a neutral K in the remaining cases. These kaons emerge from the primary vertex and are correlated in phase space with the B_s^0. They are selected requiring an impact parameter with respect to the primary vertex with a significance $\mathrm{IP}/\sigma_{\mathrm{IP}} < 2.5$, a difference in pseudo-rapidity with respect to the reconstructed B_s^0 $|\Delta\eta| < 1$, a difference in ϕ angle $|\Delta\phi| < 1.1$ and $\Delta m < 1.5$ GeV, where Δm is the difference between the mass of the $B_s^0 K$ combination and the mass of the reconstructed B_s^0. For this tag we require also $p > 4\,\mathrm{GeV}/c$ and $p_{\mathrm{T}} > 0.4\,\mathrm{GeV}/c$. In Fig. 5 the distribution of $\Delta\eta$ and Δm are shown for same-side tag kaons candidates, after $\mathrm{IP}/\sigma_{\mathrm{IP}}$, p and p_{T} cuts and have been applied, in a sample of $B_s^0 \to D_s^{\mp} K^{\pm}$ events.

As a comparison, in Fig. 6 the same variables are shown in a sample of $B^0 \to \pi^+\pi^-$ events, where no same side kaon is expected. The slight excess of wrong tag kaons which is visible in these plots, is due to kaons from the opposite b-hadron, with small impact parameter with respect to the primary vertex, which remains included in the sample.

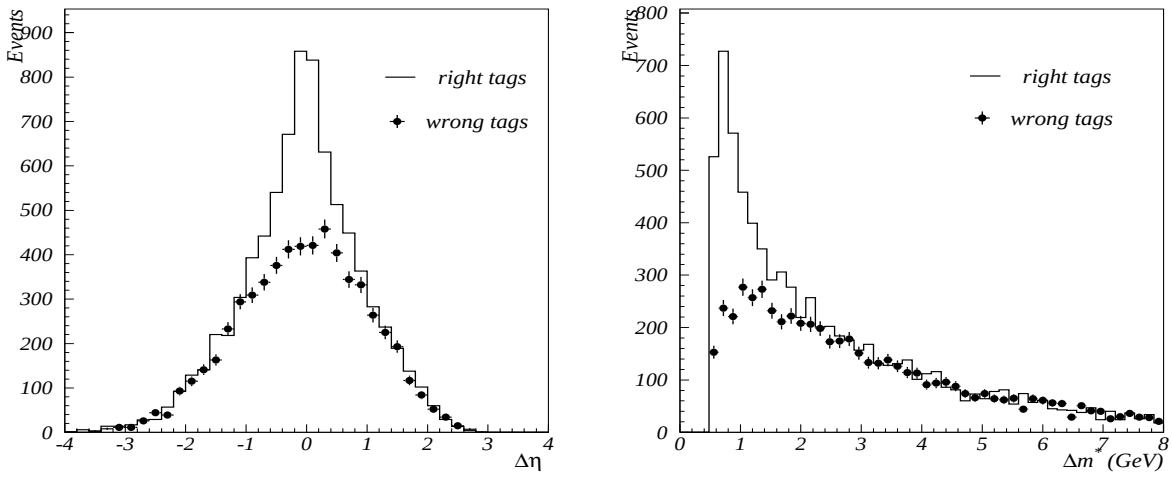

Figure 5: Distribution of the variables $\Delta\eta$ and Δm for same-side tag kaons candidates with right and wrong charge, after IP/$\sigma_{\rm IP}$, p and $p_{\rm T}$ cuts and have been applied, in a sample of $\rm B_s^0 \to D_s^{\mp} K^{\pm}$ events.

5 Inclusive reconstruction of secondary vertices and vertex charge

An inclusive reconstruction of the opposite b-hadron is performed by means of the inclusive reconstruction of secondary vertex. The reconstruction starts using two tracks as seeds. These tracks need to be reconstructed as *long* tracks and must satisfy kinematic cuts which enhance the probability to come from the b-hadron decay. Track pairs compatible with a $\rm K_S^0$ decay are also excluded. Other tracks are then included if they satisfy additional kinematic criteria on the impact parameter, χ^2 of the secondary vertex and distance from the primary vertex. Every time an additional track is included, the algorithm calculates the impact parameter of all selected tracks with respect to the vertex formed by all the other selected tracks. The track that gives the largest impact parameter significance is dropped if this value is larger than 3. A secondary vertex is found in about 49% of the events which passed Level-0 and Level-1 trigger selection, and includes on average 57% of the available b-hadron decay tracks. The mean number of tracks at the secondary vertex is 3.1, 2.6 of which are true b-hadron decay products.

Fig. 7 shows the b-hadron flight direction, determined from the primary to secondary vertex direction, using generated vertices coordinates or reconstructed vertices coordinates.

The inclusive reconstruction of the accompanying b decay vertex is used to determine the b-hadron charge. The vertex charge is defined as the sum of the charges of all tracks associated to the vertex. Fig. 8 shows the distribution of the vertex charge when the decaying b-hadron is charged. The peaks at $Q_{\rm vtx} = 0,\pm 2$ are dominated by events with vertices formed by two tracks only.

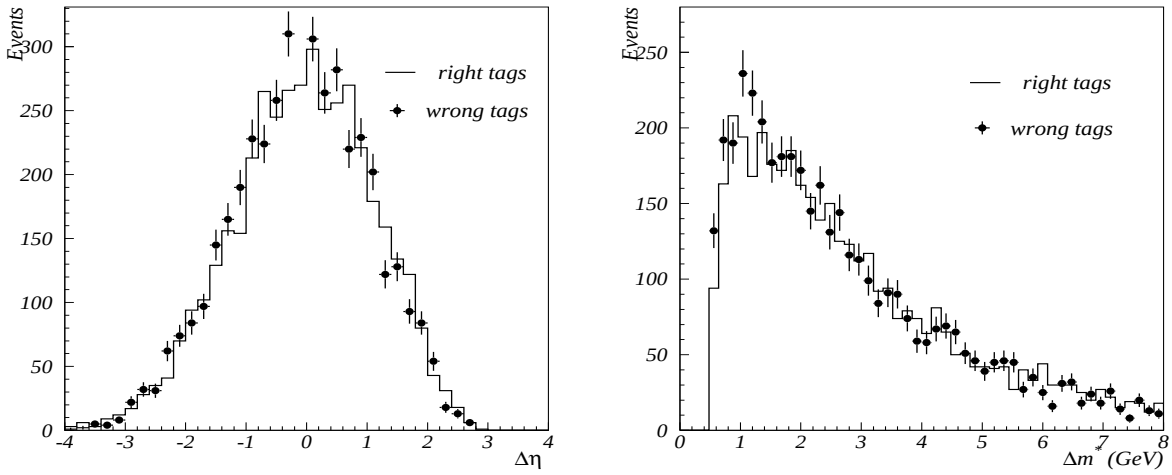

Figure 6: Distribution of the variables $\Delta\eta$ and Δm for same-side tag kaons candidates with right and wrong charge, after IP/$\sigma_{\rm IP}$, p and $p_{\rm T}$ cuts and have been applied, in a sample of $\rm B^0 \to \pi^+\pi^-$ events.

6 Results on tagging performances

The final decision on the production flavour of the reconstructed B candidate is taken using the charge of the tagging particle, or the secondary vertex charge, when only one tag is available. The same-side kaon tag is used only for $\rm B_s^0$ candidates. If there are more than one tag, the vertex charge is ignored and the final decision is taken as follows: if both the muon and the electron tag are available, the one with the highest $p_{\rm T}$ i.e. highest probability to come from a $\rm b \to \ell$ decay, is used. If two single-track tags are available and they disagree, the B candidate remains untagged. If three single-track tags are available, the decision taken by the majority of them is used.

In order to determine the performance of this combined tagging decision, events are sorted in different categories according to which tags were included in the final decision; the performance is first determined in each category, and the total effective efficiency is obtained as the sum of the effective efficiencies determined in each category separately.

Results for tagging efficiencies, wrong tag probabilities and effective efficiencies are shown in Table 5 for $\rm B_s^0 \to D_s^{\mp} K^{\pm}$ *selectable* signal decays passing the Level-0 and Level-1 trigger. The performance is shown for each tag independently, as well as for the combined tagging decision. In Table 6 the performances are shown before any trigger requirements and after Level-0 trigger only. As expected and illustrated in Table 7 the tagging performance is better in events with a single visible collision, but remains very reasonable for events with multiple collisions (27% of the events). In particular the efficiency for muons increases events with multiple collisions, due to an interplay between muon trigger and pile-up veto, while the kaon mistag probability increases due to the increase of background kaons.

Combined performance on tagging efficiencies, wrong tag probabilities and effective efficiencies for events passing the trigger and offline selection in several different channels are shown in Table 8. The performance is shown for each tag independently, as well as

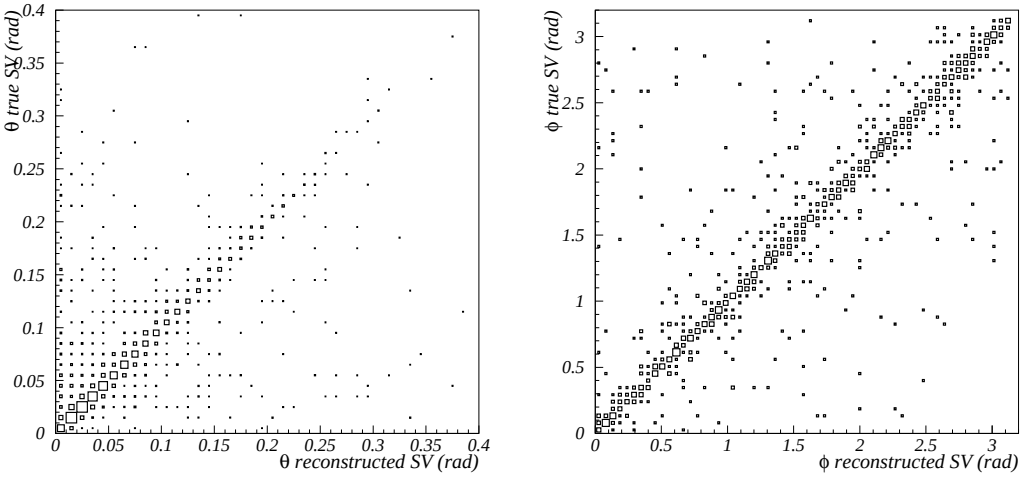

Figure 7: Opposite b-hadron flight directions, determined from the primary to secondary vertex direction, using generated vertices coordinates or reconstructed vertices coordinates.

for the combined tagging decision in Table 9 for $B^0 \to \pi^+\pi^-$, $B^0 \to K^+\pi^-$,$B_s^0 \to K^+K^-$ and $B_s^0 \to \pi^+K^-$ signal decays.

Differences occur between channels because the accompanying b-hadron is biased by the trigger, and, through the $b\bar{b}$ correlation, by the acceptance and offline selection cuts on the reconstructed B. This is shown, as an example, in Fig. 9 for the case of $B_{(s)}^0 \to h^+h^-$ selection.

The tagging performance also depends rather strongly on the $b\bar{b}$ production mechanism, as different processes produce different $b\bar{b}$ correlations (see Table 10) Fig. 10 shows, for the different processes types used in the PYTHIA generation, the p_T distribution of the opposite b-hadron and the difference in azimuthal angle between the two b-hadrons. For example, when a $b\bar{b}$ pair is produced back-to-back as in $g + g \to f + \bar{f}$, the b hadrons tend to be more cleanly separated in azimuthal angle, and this improves the tagging performance for this particular process. Events used for Fig. 10 and Table 10 are $B_s^0 \to D_s^{\mp}K^{\pm}$ *selectable* signal decays, single-collision, passing the Level-0 and Level-1 trigger.

Differences in tagging performance between a reconstructed B containing a $\bar{b}$ at production and a reconstructed B containing a b quark at production have been examined with the $B^0 \to J/\psi K^{*0}$ channel and found to be smaller than 0.9%, consistent with zero with the present MC statistics.

All results presented in this note use the truth information to determine whether a tag is correct or not, and the quoted uncertainties on the performance arise from the present Monte Carlo statistics. In order to reduce the dependence on the Monte Carlo, it will be possible, in an real physics analysis, to determine the wrong tag fractions directly from the data. This can be done for decays to flavour-specific final states by measuring the amplitude of the B^0 or B_s^0 oscillations, i.e. of the $\cos(\Delta m\, t)$ term in the mixing asymmetry. However, this is not possible for a non flavour-specific channel (e.g. $B^0 \to J/\psi K_S^0$ or $B_s^0 \to D_s^{\mp}K^{\pm}$); in this case, we will be able to use another channel with the same topology ($B^0 \to J/\psi K^{*0}$ or $B_s^0 \to D_s^-\pi^+$ in our examples) for which the trigger

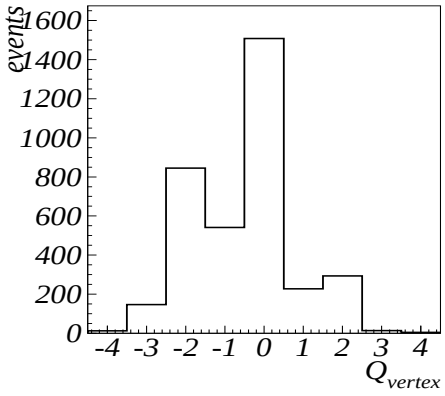

Figure 8: Vertex charge distribution when the decaying b-hadron is a B^-.

and the selection have a very similar response and hence introduce the same bias on the tagging performance.

7 Conclusions and Outlook

Results on flavour tagging in LHCb has been presented, using same side and opposite side algorithms. Same-side tagging of B^0 mesons using soft pions, successfully applied in the past at CDF, is under study and may be added in the future. A new approach is also under study, to be applied to the different tagging algorithms, which use a Neural-Net the better exploit the correlation amongst all the analysis variables. Preliminary but promising results, not shown in the present note, have been obtained with this technique and will explored further in the near future.

tag	$\varepsilon_{\rm tag}(\%)$	$w(\%)$	$\varepsilon_{\rm eff}(\%)$	tag	$\varepsilon_{\rm tag}(\%)$	$w(\%)$	$\varepsilon_{\rm eff}(\%)$
μ	14.5±0.2	34.4±0.8	1.42±0.14	μ	8.9	33.	0.96
				μ, K_{opp}	1.6	21.	0.52
				μ, K_{same}	1.2	18.	0.47
e	6.2±0.1	34.1±1.2	0.62±0.10	e	3.5	31.	0.52
				e, K_{opp}	0.70	23.	0.20
				e, K_{same}	0.48	17.	0.21
K_{opp}	20.1±0.3	32.9±0.6	2.34±0.18	K_{opp}	11.6	33.	1.27
				K_{opp},K_{same}	1.7	17.	0.76
K_{same}	17.9±0.3	29.7±0.7	2.97±0.20	K_{same}	11.6	30.	1.88
				μ,K_{opp},K_{same}	0.6	28.	0.12
				e,K_{opp}, K_{same}	0.2	30.	0.04
$Q_{\rm vtx}$	27.9±0.3	41.3±0.5	0.84±0.11	$Q_{\rm vtx}$	12.4	43.6	0.20
				Combined	54.4±0.4	31.9±0.3	7.15±0.31

Table 5: Tagging performance for $B_s^0 \to D_s^{\mp} K^{\pm}$ signal events passing L0 and L1 trigger cuts. Uncertainties are statistical.

	no trigger			L0 trigger		
tag	$\varepsilon_{\rm tag}(\%)$	$w(\%)$	$\varepsilon_{\rm eff}(\%)$	$\varepsilon_{\rm tag}(\%)$	$w(\%)$	$\varepsilon_{\rm eff}(\%)$
μ	6.7±0.1	34.8±0.5	0.62±0.04	11.7±0.1	33.3±0.6	1.30±0.1
e	4.3±0.1	34.6±0.6	0.41±0.03	5.1±0.1	35.7±0.9	0.41±0.05
K_{opp}	17.0±0.1	36.0±0.3	1.33±0.06	17.3±0.2	33.9±0.5	1.78±0.11
K_{same}	15.2±0.1	30.8±0.3	2.23±0.08	17.4±0.2	29.7±0.5	2.87±0.13
$Q_{\rm vtx}$	23.7±0.1	42.1±0.3	0.59±0.04	24.1±0.2	41.9±0.4	0.63±0.07
Combined	45.4±0.2	34.2±0.2	4.6±0.1	49.6±0.3	32.2±0.2	6.3±0.2

Table 6: Tagging performance for $B_s^0 \to D_s^{\mp} K^{\pm}$ signal events before trigger cuts and after L0 trigger cuts. Uncertainties are statistical.

	single collision			multiple collision		
tag	$\varepsilon_{\rm tag}(\%)$	$w(\%)$	$\varepsilon_{\rm eff}(\%)$ tag	$\varepsilon_{\rm tag}(\%)$	$w(\%)$	$\varepsilon_{\rm eff}(\%)$
μ	12.7±0.3	34.8±1.0	1.2±0.2	19.4±0.5	33.7±1.2	2.1±0.3
e	6.2±0.2	32.7±1.4	0.8±0.1	5.8±0.3	38.0±2.4	0.3±0.1
K_{opp}	18.9±0.3	30.9±0.8	2.8±0.2	23.4±0.5	37.3±1.1	1.5±0.3
K_{same}	18.5±0.3	29.7±0.8	3.0±0.2	16.4±0.5	29.4±1.3	2.8±0.4
$Q_{\rm vtx}$	26.2±0.4	40.2±0.7	1.0±0.2	32.4±0.6	43.9±1.0	0.5±0.2
Combined	56.3±0.5	31.7±0.4	7.5±0.4	58.4±0.8	31.7±0.4	6.6±0.6

Table 7: Tagging performance for $B_s^0 \to D_s^{\mp} K^{\pm}$ signal events after trigger cuts for events with a single collision and multiple collisions. Uncertainties are statistical.

Channel	$\varepsilon_{\rm tag}$ (%)	w (%)	$\varepsilon_{\rm eff}$ (%)
$B^0 \to \pi^+\pi^-$	41.8±0.7	34.9±1.1	3.8±0.5
$B^0 \to K^+\pi^-$	43.2±1.4	33.3±2.1	4.8±1.0
$B^0 \to J/\psi(\mu\mu)K^0_S$	45.1±1.3	36.7±1.9	3.2±0.8
$B^0 \to J/\psi(\mu\mu)K^{*0}$	41.9±0.5	34.3±0.7	4.1±0.3
$B^0_s \to K^+K^-$	49.8±0.5	33.0±0.8	5.8±0.5
$B^0_s \to \pi^+K^-$	49.5±1.8	30.4±2.6	7.6±1.7
$B^0_s \to D^-_s\pi^+$	54.6±1.2	30.0±1.6	8.7±1.2
$B^0_s \to D^\mp_s K^\pm$	54.2±0.6	33.4±0.8	6.0±0.5
$B^0_s \to J/\psi(\mu\mu)\phi$	50.4±0.3	33.4±0.4	5.5±0.3

Table 8: Performance of the combined tag for different signal decays passing trigger and offline cuts. Uncertainties are statistical.

tag	$\varepsilon_{\rm tag}$ (%)	w (%)	$\varepsilon_{\rm eff}$ (%)
μ	11.1±0.3	35.3±1.1	1.0±0.2
e	5.2±0.2	35.6±1.7	0.4±0.1
$K_{\rm opp}$	16.6±0.3	31.2±0.9	2.4±0.2
$Q_{\rm vtx}$	24.3±0.6	39.9±0.8	1.0±0.2
Combined (B^0)	40.9±0.4	34.6±0.7	3.9±0.3
$K_{\rm same}$	17.5±0.4	32.8±1.2	2.1±0.3
Combined (B^0_s)	49.8±0.5	32.8±0.8	5.9±0.5

Table 9: Tagging performance for $B^0_{(s)} \to h^+h^-$ signal events passing trigger and offline cuts. Uncertainties are statistical.

Sample	fraction	$\varepsilon_{\rm eff}$ (%)
All		7.1 ± 0.3
$f + f \to f + f$	9%	7.5 ± 1.2
$f + g \to f + g$	45%	6.5 ± 0.5
$g + g \to f + \bar{f}$	18%	10.2 ± 1.0
$g + g \to g + g$	27%	8.0 ± 0.7

Table 10: Effective tagging efficiency for different sub-samples of $B^0_s \to D^\mp_s K^\pm$ events (after trigger but before offline cuts), defined by the PYTHIA process type (for single-collision events).

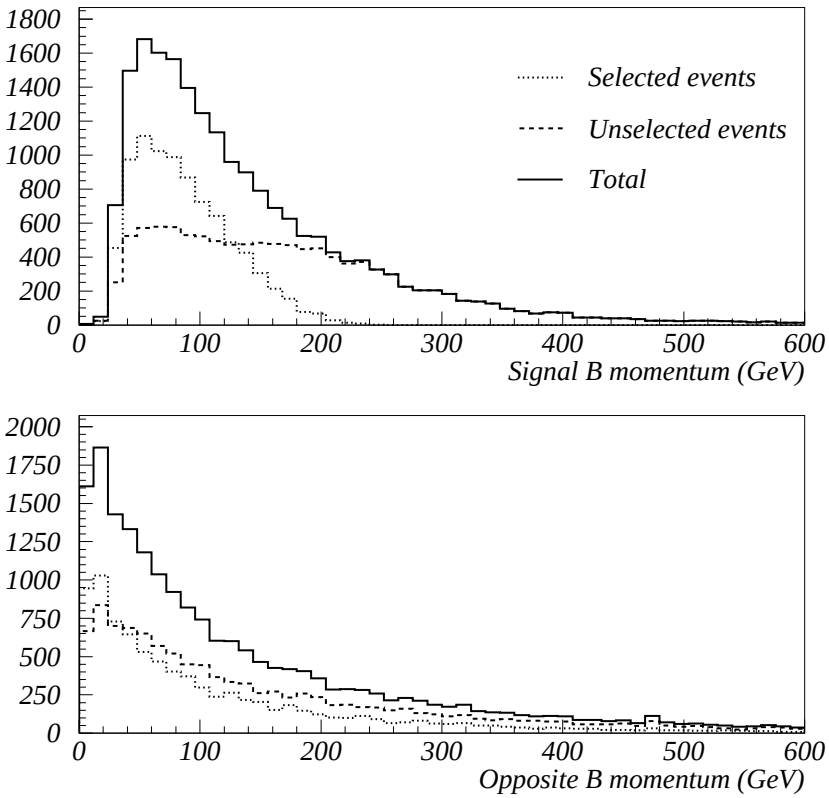

Figure 9: p_{T} distribution of the signal B-meson and of the opposite b-hadron for events which are *selectable* (continuous line) and off-line selected (dotted line) or off-line not selected (dashed line). Events are $\mathrm{B}^0_{(\mathrm{s})} \to \mathrm{h}^+\mathrm{h}^-$.

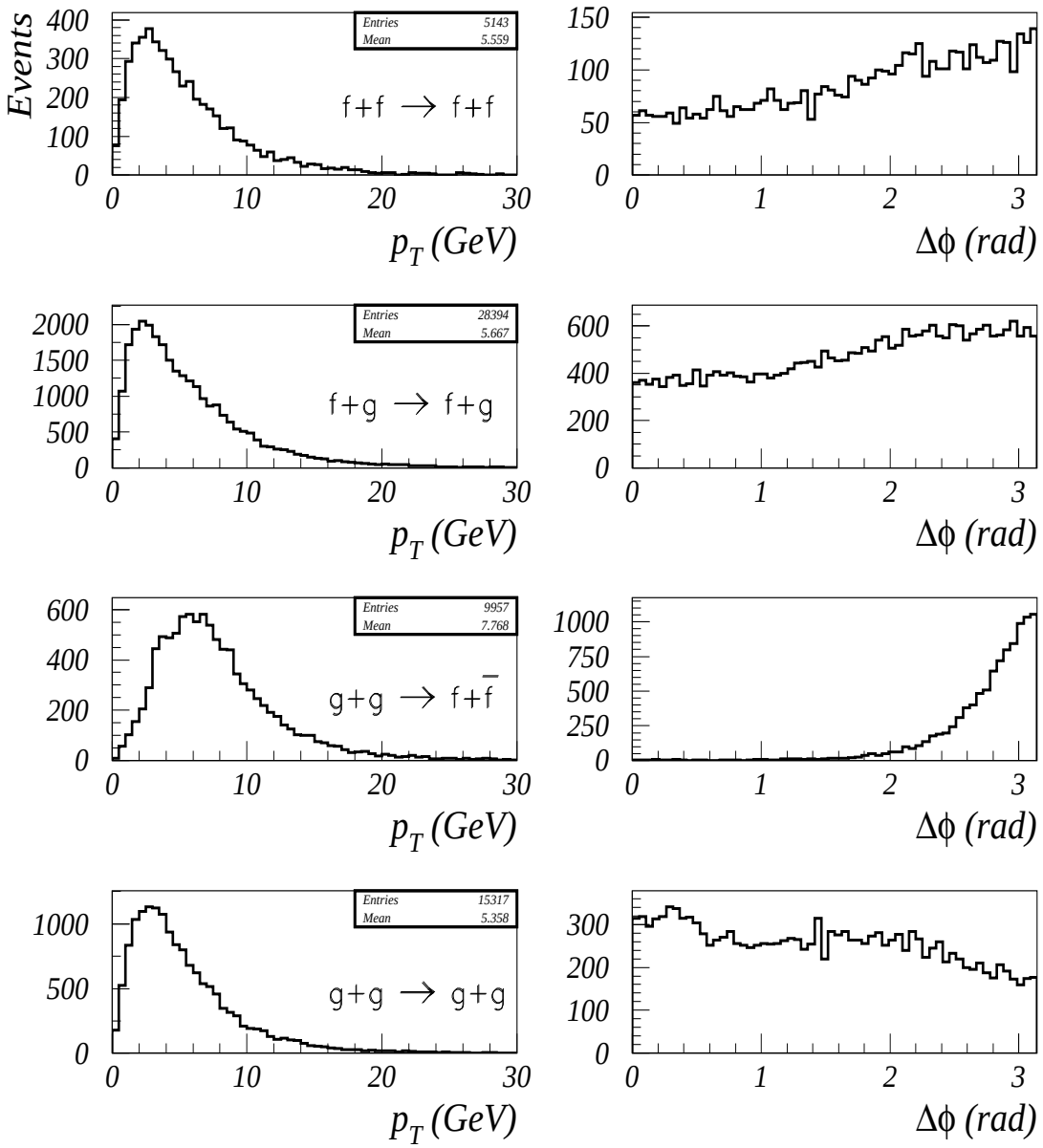

Figure 10: p_{T} distribution of the opposite b-hadron and difference in azimuthal angle between the two b-hadrons, for the different processes used in the PYTHIA generation.